Applied Clay Science 107 (2015) 145–155

Contents lists available at ScienceDirect

Applied Clay Science

journal homepage: www.elsevier.com/locate/clay

Research paper

Pre-historic production of ceramics in the Amazon: Provenience, raw materials, and firing temperatures

Suyanne Flavia Santos Rodrigues [a,*], Marcondes Lima da Costa [a,1], Herbert Pöllmann [b,2], Dirse Clara Kern [c,3], Maura Imazio da Silveira [c,3], Renato Kipnis [d,4]

[a] Federal University of Pará, Augusto Correa Street, 1 Guamá, Belém, Pará 66110075, Brazil
[b] University of Halle, Von Seckendorff Platz 3, D-06120 Halle (Saale), Germany
[c] Emilio Goeldi Paraense Museum, Perimetral Avenue, 1901, Terra Firme, Belém, Pará 66077-830, Brazil
[d] University of São Paulo, Matão Street, 277, São Paulo, São Paulo 05508-900, Brazil

ARTICLE INFO

Article history:
Received 28 August 2014
Received in revised form 15 January 2015
Accepted 18 January 2015
Available online 3 February 2015

Keywords:
Sherds
Non-plastic materials
Crushed rocks
Shells
Cariapé
Amazon region

ABSTRACT

The chemical–mineralogical properties of prehistoric ceramics found in the Amazon were investigated with the aim of elucidating the production technology, the raw materials used, and the origin of these materials. For this, sherds were obtained from three archeological sites located in distinct regions of the basin. The mineralogical composition of the samples was determined by X-ray diffraction, optical microscopy, thermal analyses, FT-IR, and SEM-EDS, while the chemical composition was measured using ICP-OES and ICP-MS. The manufacturing process consisted of the coiling technique with the smoothing of surfaces, and the addition of organic and mineral non-plastic materials. The pots were fired at ±600 °C, leading to the formation of an amorphous metakaolinite matrix in which a number of different types of non-plastic materials can be found. These non-plastic materials, together with the phosphates found in the samples, represent the principal differences in the chemical and mineralogical composition of the sherds from different sites. The raw material (clay) used for the production of the ceramic sherds from the Da Mata and Jabuti sites had the same geological origin, and were distinct from those of Monte Dourado 1 in relation to the intensive use of crushed rock. Cariapé was found throughout the region, and the shells reflect the proximity of the Jabuti site to the ocean. The phosphates found in the matrix probably formed during the use of the pots to prepare food, and could not have been part of the raw material, given that they would not have resisted the firing temperature. The evidence indicates that the potters used the materials available locally for the production of ceramics. The use of cariapé at all the sites confirmed that this practice was widespread in the region, representing an important cultural trait of the production of ceramics in the prehistoric Amazon.

1. Introduction

In archeological studies, ceramic objects represent an important investigative tool, and the analysis of samples can provide important insights into the origin of the raw materials (clays, non-plastic materials) (Dias et al., 2013; Prudêncio et al., 2006, 2009), possible commercial and cultural interchanges among communities, evidence on technological differences (e.g., modeling, coiling, and throwing), as well as the firing temperatures, based on the mineralogical transformations occurring during the manufacture of the items (Iordanidis et al., 2009; Mohamed et al., 2010; Trindade et al., 2010, 2011). Chemical and mineralogical analyses of samples are used to evaluate these parameters, and have been applied to sherds retrieved from a wide range of archeological sites, especially in Europe (Fermo et al., 2008; Gimenez et al., 2006; Hein et al., 2004; Iordanidis and Garcia-Guinea, 2011; Kramar et al., 2012; Maritan et al., 2013; Montana et al., 2011; Moropoulou et al., 1995; Papadopoulou et al., 2004; Rathossi and Pontikes, 2010; Romani et al., 2000).

In the Amazon, similar studies have been and are being developed, although perspectives on the diversity of raw materials, manufacturing techniques and firing temperatures are still limited (Costa et al., 2004a, b, 2009, 2011, 2012). Studies of anthropogenic soils, especially Amazonian Dark Earth (ADE) are far more numerous (Costa and Kern, 1999; Costa et al., 2013; Glaser et al., 2001; Kern and Kämpf, 1989; Lehmann et al., 2003; Lemos et al., 2011; Lima et al., 2002; Mescouto et al., 2011; Schmidt et al., 2014; Silveira et al., 2011; Smith, 1980; Woods et al., 2009).

* Corresponding author. Tel.: +55 9132017428.
E-mail addresses: suyanneflavia@gmail.com (S.F.S. Rodrigues), marcondeslc@gmail.com (M.L. Costa), herbert.poellmann@geo.uni-halle.de (H. Pöllmann), kern@museu-goeldi.br (D.C. Kern), mauraslvr@yahoo.com (M.I. Silveira), rkipnis@scientiaconsultoria.com.br (R. Kipnis).
[1] Tel.: +55 9132017428.
[2] Tel.: +49 345 55 26164.
[3] Tel.: +55 913075 6272.
[4] Tel.: +55 1130917725.

http://dx.doi.org/10.1016/j.clay.2015.01.016
0169-1317/

Given these shortcomings, the present study investigated the production of archeological ceramics in the Amazon, with regard to the origin of raw materials (clay and non-plastic materials), the manufacturing processes, and firing temperatures through the chemical and mineralogical characterization of samples from different sites, in order to evaluate the potential technological variation in the productive process in distinct pottery-making populations, providing new insights into the complexity of the prehistoric occupation of the Amazon.

2. Materials and methods

2.1. Materials

For the present study, sherd vessels were obtained from three archeological sites in the Brazilian Amazon – Monte Dourado 1, Jabuti and Da Mata (Fig. 1) – based on their geographical distribution and the availability of material for analysis. All the samples were representative of the sides of the pots and were not embossed or painted.

2.1.1. Monte Dourado 1

The Monte Dourado 1 site (central coordinates: UTM 22M 329403/9928604) is located on the right margin of the Jari River, in the district of Monte Dourado, part of the municipality of Almeirim and in the Brazilian state of Pará. The samples from this site (CF-MD1) were collected by Scientia Scientific Consultants Ltd. in May, 2011, and were kindly provided for the present study by this company.

Monte Dourado 1 is a habitation site with Amazonian Dark Earth (ADE) deposits containing high densities of ceramics and smaller quantities of stone tools. This site covers a total area of 235,200 m^2 (560 m × 420 m), delimited using 401 boreholes. The ADE horizon reaches a depth of 70 cm in some places. The excavations were conducted in artificial layers of 10 cm until no more archeological remains were encountered (Scientia, 2011). The results of the analysis of the style of pottery found at this site have not yet been made available.

2.1.2. Da Mata

The Da Mata site (central coordinates: UTM 22M 595850/9715416) is located in the municipality of São José do Ribamar, in the eastern extreme of São Luís Island, in São José Bay and in the Brazilian state of Maranhão. The samples from this site (CF-DM) were also collected by Scientia Scientific Consultants Ltd. in 2009, under the supervision of Dra. Dirse Clara Kern, who kindly provided the material for the present study.

Da Mata is a cemetery and habitation site, which was delimited using 132 boreholes, of which, 68 produced archeological material. The ADE horizon extended from the surface to a depth of 30 cm. The excavations were conducted in artificial layers of 10 cm until no further archeological remains were encountered (Scientia, 2009). As for the Monte Dourado 1 samples, information on the pottery style is still unavailable.

2.1.3. Jabuti

The Jabuti site (central coordinates: UTM 22M 0550771/9358220) is located on the Atlantic coast of the municipality of Bragança in northeastern Pará. The samples from this site (CF-JAB) were collected by a team of archeologists from the Emilio Goeldi Paraense Museum in Belém coordinated by Dra. Maura Imazio da Silveira.

This site is also of the habitation type, and is characterized by a number of patches of ADE, with depths ranging from 60 cm to more than 1 m in places, and large quantities of ceramic material distributed on the surface and lower down. The excavations were conducted in artificial layers of 20 cm until archeological remains were absent. The pottery is of the Mina tradition, described by Simões (1981), and typical of the sambaqui middens of the Amazon region (Silveira et al., 2011).

2.2. Methods

The samples (Table 1) were dried at ambient temperature, and then the attached allochthonous substrate and products of weathering were removed carefully with distilled water. Due to the large amount of material, the sherds from Monte Dourado and Jabuti were subdivided to obtain a sample of 300 g for each site, which was equivalent to the sample collected from the Da Mata site. The samples were classified by thickness, based on the criteria established by Alves (1988), Rye (1981), Braun (1983) and Schiffer et al. (1994), which are normally used for the classification of archeological ceramics. All the sherds analyzed in the present study were either 9 mm thick or less, and were thus classified as thin or very thin, or were at least 12 mm thick, being recorded as medium or thick. The thickness of the samples is an important parameter here, given that the evidence indicates that the thinnest pots were used for cooking.

Following cleaning and the classification of the sherds by their thickness, the sherds were described mesoscopically using a ZEISS-Stemi 2000-C stereomicroscope and photographed with an attached Canon PowerShot G6 camera. During this examination, the coloration of the samples (based on the Munsell color system), their texture, and the non-plastic materials they contained were identified and recorded. Samples were then selected for the mineralogical study using optical and electron microscopy, while the rest of the material

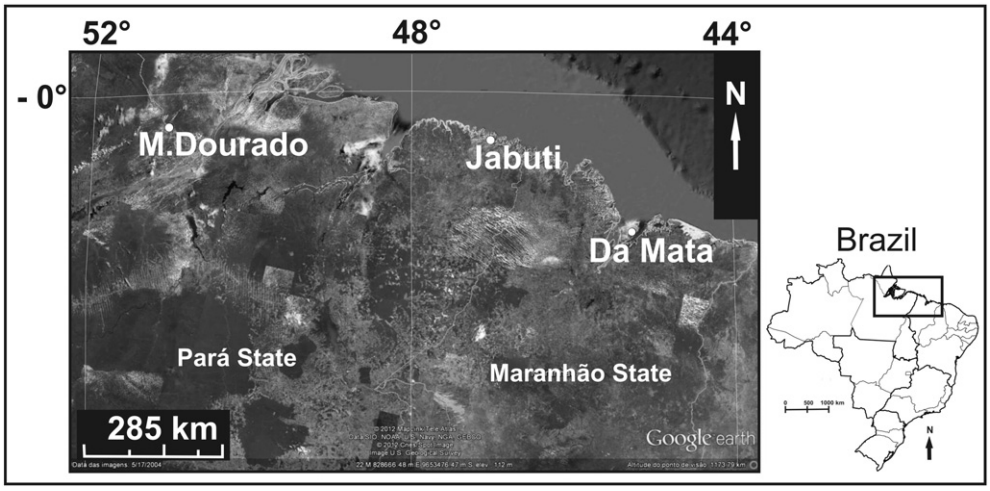

Fig. 1. Localization of Monte Dourado 1, Da Mata and Jabuti sites.

Table 1
Description of the sherds analyzed from Monte Dourado 1, Da Mata and Jabuti archeological sites. (*) Most common non-plastic.

Samples	Depth (cm)	Non-plastic	Surface color (Munsell color chart)	Manufacture technique after external aspects	n
Monte Dourado 1					
CF-MD1 9 a	0–10	Mineral* + cariapé	(5YR4/3)	Coil technique/ smooth on the surface	22
CF-MD1 12 a	0–10	Mineral* + cariapé	(5YR4/3)	Coil technique/ smooth on the surface	3
CF-MD1 9 b	10–20	Mineral* + cariapé	(5YR4/3)	Coil technique/ smooth on the surface	19
CF-MD1 9 b	10–20	Mineral* + cariapé	(5YR4/3)	Coil technique/ smooth on the surface	3
CF-MD1 12 c	20–30	Mineral* + cariapé	(5YR4/3)	Coil technique/ smooth on the surface	13
CF-MD1 12 c	20–30	Mineral* + cariapé	(5YR4/3)	Coil technique/ smooth on the surface	3
CF-MD1 9 d	30–40	Mineral* + cariapé	(5YR4/3)	Coil technique/ smooth on the surface	13
CF-MD1 12 d	30–40	Mineral* + cariapé	(5YR4/3)	Coil technique/ smooth on the surface	4
CF-MD1 9 e	40–50	Mineral* + cariapé	(5YR4/3)	Coil technique/ smooth on the surface es	16
CF-MD1 12 e	40–50	Mineral* + cariapé	(5YR4/3)	Coil technique/ smooth on the surface	4
CF-MD1 9 f	50–60	Mineral* + cariapé	(5YR4/3)	Coil technique/ smooth on the surface	14
CF-MD1 12 f	50–60	Mineral* + cariapé	(5YR4/3)	Coil technique/ smooth on the surface	4
CF-MD1 9 g	60–70	Mineral* + cariapé	(5YR4/3)	Coil technique/ smooth on the surface	13
CF-MD1 12 g	60–70	Mineral* + cariapé	(5YR4/3)	Coil technique/ smooth on the surface	5
M. Dourado ≤ 9 mm					110
M. Dourado ≥ 12 mm					26
Total					136
Da Mata					
CF-DM 9 a	0–10	Cariapé	(5YR5/4)	Coil technique/ smooth on the surface	14
CF-DM 12 a	0–10	Cariapé	(5YR5/4)	Coil technique/ smooth on the surface	8
CF-DM 9 b	10–20	Cariapé	(5YR5/4)	Coil technique/ smooth on the surface	28
CF-DM 12 b	10–20	Cariapé	(5YR5/4)	Coil technique/ smooth on the surface	10
CF-DM 9 c	20–30	Cariapé	(5YR5/4)	Coil technique/ smooth on the surface	18
CF-DM 12 c	20–30	Cariapé	(5YR5/4)	Coil technique/ smooth on the surface	8
CF-DM 9 d	30–40	Cariapé	(5YR5/4)	Coil technique/ smooth on the surface	14
CF-DM 12 d	30–40	Cariapé	(5YR5/4)	Coil technique/ smooth on the surface	12
CF-DM 9 e	40–50	Cariapé	(5YR5/4)	Coil technique/ smooth on the surface	16
CF-DM 12 e	40–50	Cariapé	(5YR5/4)	Coil technique/ smooth on the surface	9
Da Mata ≤ 9 mm					90
Da Mata ≥ 12 mm					47
Total					137
Jabuti					
CF-JAB a	0–10	Shell* + cariapé	(5YR5/2)	Not identified	5
CF-JAB bc	10–30	Shell* + cariapé	(5YR5/2)	Not identified	4
CF-JAB de	30–50	Shell	(5YR5/2)	Not identified	4
CF-JAB fg	50–70	Shell	(5YR5/2)	Not identified	11
CF-JAB h	70–90	Shell	(5YR5/2)	Not identified	4
CF-JAB i	90–110	Shell	(5YR5/2)	Not identified	5
CF-JAB j	110–130	Shell	(5YR5/2)	Not identified	5
CF-JAB l	130–150	Shell	(5YR5/2)	Not identified	7
CF-JAB m	150–70	Shell	(5YR5/2)	Not identified	7
Total					52

was ground in an agate mortar for the additional chemical and mineralogical analyses.

The micro-textural characteristics of the ceramic sherds were determined using a Carl Zeiss Axiolab 450910 petrographic microscope, with the samples placed on thin slides without coverslips. This procedure was complemented by semi-quantitative chemical analyses complemented by scanning electron microscopy coupled to an energy-dispersive X-ray spectrometry system (SEM-EDS), using a LEO

1450VP microscope with a voltage of 17.5 kV and a Gresham EDS detector equipped with a Be window and Q500 multi-channel analyzer. The samples were metalized with Au and the analyses were run using the IXRF software in the UFPA electronic microscopy laboratory.

The mineral components of the samples were identified by X-ray diffraction (XRD), using the powder method. For this, the samples were ground in an agate mortar and compacted in a sample holder for processing in an XPERT PRO MPD diffractometer with a PW 3040/60 (theta-theta) PANalytical goniometer, copper anode (λCuKα1 = 1.54060), Kβ filter, 40 kV tension generator and 30 mA current generator. The scanning interval was 5–75°, which encompasses the principal peak characteristic of the target minerals. The analyses had a step of 0.0170 (2θ) and a step time of 10.3377 s, and a fixed divergent gap of 0.2393 mm. These analyses were conducted in the UFPA Mineral Characterization Laboratory.

Thermogravimetric and thermodifferential analyses were conducted on subsamples of 0.02 g of the pulverized material, to investigate the thermal behavior of the ceramic sherds. The assays were run at temperatures of up to 1100 °C, with a heating rate of 10 °C/min in an inert atmosphere (N_2), using a PL Thermal Sciences thermo-analyzer simultaneously with an STA 1000/1500 analyzer (Stanton Redcroft Ltd.), in the UFPA mineral characterization laboratory.

The same samples were then analyzed using an FT-IV absorption spectroscope (FT-IR) to confirm the presence of amorphous and crystalline phases, and organic matter. For this, a compressed pellet of each pulverized sample was prepared from 0.0015 g of the sample and 0.2 g of Potassium bromide (KBr), under a pressure of 1.8 Kbar. The analysis was conducted using a Vertex 70 Bruker spectrometer with a spectral range of 400–4000 cm^{-1}, with measurements taken at every 4 cm^{-1}, in the UFPA Mineralogy, Geochemistry and Applications Laboratory.

The chemical composition representative of the total sample (major, minor, and trace elements) was obtained by Inductively Coupled Plasma Mass Spectrometry (ICP-MS Perkin Elmer Elan 9000) and Inductively Coupled Plasma Emission Spectroscopy (ICP-OES Varian) by AcmeLabs. For this, the pulverized samples were prepared by fusion with lithium tetraborate (Anachemia Science) followed by dilution in nitric acid (Merck). The Loss on Ignition (LOI) was determined by gravimetry, which consists of the measurement of the mass following calcination at 1000 °C, procedure also conducted by AcmeLabs.

3. Results

3.1. Non-plastic materials

The non-plastic materials found in the different ceramic samples included cariapé, shell, and ground rock, depending on the site from which the sample was obtained. Only cariapé was found in the Da Mata samples (Fig. 2b). At Jabuti, most samples contained only shell fragments (Fig. 2c), although those found at a depth of 60 cm contained a combination of shell and cariapé. At Monte Dourado 1, the cariapé was combined with crushed rock (Fig. 2a).

Cariapé is derived from the bark of trees of the species *Licania utilis* and the genus *Moquilea* (Linné, 1925), which are widely distributed in the Amazon, and are still used for this purpose by traditional populations (Linné, 1925; Meggers and Evans, 1957). To prepare the temper, the bark is pulverized and calcined to produce amorphous siliceous ash, sometimes in the form of tridymite–cristobalite (Costa et al., 2004b, 2011).

The mineral non-plastic identified in the Monte Dourado 1 samples was composed primarily of fragments of ground rock containing quartz, ilmenite, plagioclases, cordierite, and cristobalite, identified by XRD. It is important to note here that the cristobalite may be related to the cariapé, given that amorphous silica may crystallize into cristobalite during firing (Costa et al., 2004b, 2011).

Grains and fragments of quartz were found in all the samples (Fig. 2) and may have been added intentionally as a temper, but would also have been a principal component of the raw material, which hampers the identification of what material was added to the clay. The quartz grains vary considerably in size and shape, although they are generally sub-angular and distributed evenly within the clay matrix. The grains were coarser in the samples from Monte Dourado 1.

3.2. The matrix

3.2.1. Metakaolinite

The principal phase of the basic matrix of the ceramic samples was metakaolinite. The backgrounds of the XRD patterns are indicative of large amounts of amorphous phases (Fig. 2), which were interpreted as being indicators of the presence of metakaolinite, given that the principal mineral of the raw material used for the production of the pots was kaolinite, and when it is calcined at low temperatures (550–600 °C), it becomes amorphous.

The metakaolinite thus constitutes the fundamental matrix, the principal component of the amorphous to crystalline brown porous mass of the ceramics (Fig. 2). The presence of metakaolinite is also indicated by the aluminosilicate characteristics of the matrix found in the SEM/EDS spot analyses (Fig. 3), as well as the mullite formation when the fragments were burned at 950 °C, as shown in curves TG/DTA (Fig. 3).

3.2.2. Quartz

Quartz is the second most important phase found in the samples, observed through both the mesoscopic and microscopic analyses, and confirmed by XRD (Fig. 2). The quartz is distributed throughout the metakaolinite matrix, being both a component of the clay raw material and the temper.

3.2.3. Muscovite

This mineral was rarely observed under optical microscopy, but was confirmed as an accessory mineral by XRD in all the samples (Fig. 2). It is present in tiny platelets distributed throughout the metakaolinite matrix, probably as a component of the clay raw material. It is also possible that this mineral was introduced into the ceramics from Monte Dourado 1 as part of the rock temper used at this site.

3.2.4. Iron oxy-hydroxides

Nodules of iron oxide, approximately 500 μm in diameter (Fig. 1), were found in all the samples, and were also present in the brown spots observed in the metakaolinite matrix. These features certainly represent the abundant brown and red spots found in the original clayey raw material.

3.2.5. Anatase

Anatase was identified only by XRD and is probably found in nanocrystals within the matrix of the Jabuti and Da Mata samples (Fig. 2). This mineral is commonly found in the latosols and lateritic formations that are so abundant in the Amazon region. It seems likely that the mottled clays of these lateritic profiles were used as the raw material for the manufacture of the original ceramic pots from which the sherds analyzed in the present study were derived. Anatase is much less common in the region's sedimentary rocks.

3.2.6. Phosphates

Phosphates, principally of aluminum, were common accessories in the ceramic archeological from Amazons, but were generally amorphous, and only rarely found in cryptocrystalline forms, such as variscite–strengite and, more rarely, rhabdophane (Costa et al., 2004b, 2006, 2011). In the samples analyzed, the aluminum phosphates are accessory and equally amorphous. However, in the Jabuti samples, they were present as microcrystalline crandallite–goyazite, observed

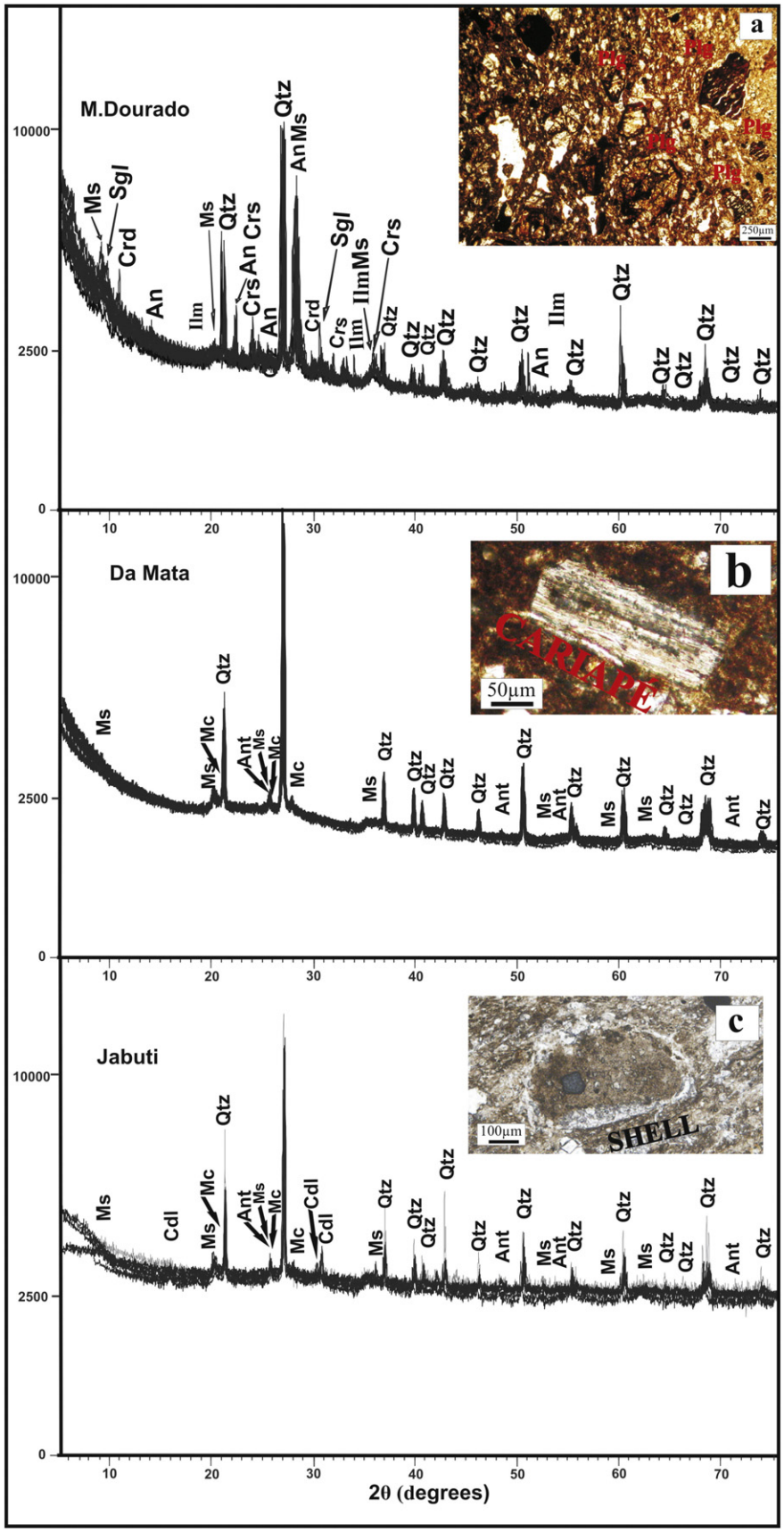

Fig. 2. Mineralogical composition of the sherds from Monte Dourado 1, Da Mata and Jabuti archeological sites by XRD powder analysis and photomicrographs showing different non-plastic materials. Optical microscope, plane polarized light, with 10× lens; Qtz = quartz; Crd = cordierite; Ms = muscovite; Cld = crandallite–goyazite; Ant = anatase; Crs = cristobalite; Ilm = ilmenite; Mc = feldspar; An = plagioclases.

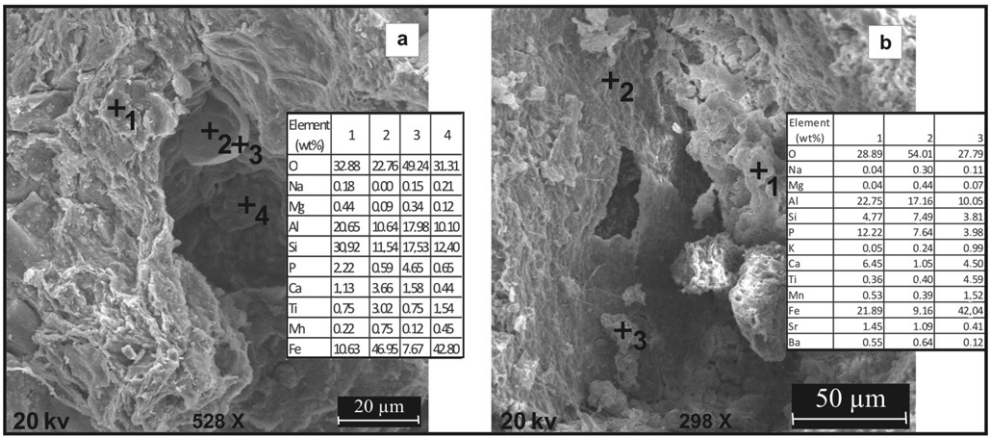

Fig. 3. Scanning electromicrographs and chemical spot analyses conducted by SEM/EDS. Samples from (a) Jabuti and (b) Monte Dourado 1.

in large quantities by XRD (Fig. 2). The presence of this mineral was confirmed by an endothermic peak in the thermograms of the samples at 440 °C (Fig. 4), which indicates the dehydroxylation of the mineral (Gilkes and Palmer, 1983) and consequent loss of crystallinity.

The SEM/EDS spot analyses revealed that the crandallite–goyazite substituted the shell fragments (Fig. 3). At the other sites, however, the phosphates were found in the pores of the matrix, and in the contact zones between these pores and the temper (Fig. 3). Stoichiometric calculations and SEM/EDS spot analyses of chemicals also allowed the presence of amorphous aluminum phosphates to be inferred in the metakaolinite matrix. This same approach, associated with the FT-IR (Fig. 4b) and the total chemical analyses (Table 2), resulted in the identification of these minerals in the ceramic sherds from Da Mata, albeit in much smaller quantities. These phosphates can be recognized by the anti-symmetric stretching of the P–O, 1035 cm^{-1} (Breitinger et al., 2006) found in the ceramic sherds from all the sites, and equivalent to variscite. Segelerite ($CaMgFe(PO_4)_2(OH)\cdot 4(H_2O)$) was also identified by XRD in the sherds from Monte Dourado 1 (Fig. 2), although the endothermic dehydroxylation peak found at 400 °C (Hochleitner and Fehr, 2010) was not observed in the thermograms (Fig. 4a), presumably as a result of its low concentration, as confirmed by the chemical data. Beyond the stretches referring to P–O, the FT-IR spectra exhibited the stretching of the O–H of the adsorbed water related to the humid content (~3430 cm^{-1}) found in the spectra of all the sherds (Fig. 4b). In addition, bands of Si–O and Si–O–Al stretching related to the silicates identified by XRD (Madejová and Komadel, 2001) were found in the sherds from all three sites.

4. Discussion

4.1. Raw materials and mineral transformation in firing manufacture of the vessels

Metakaolinite and quartz were the principal components of sherds retrieved from other archeological sites in the Brazilian Amazon (Costa et al., 2004b, 2011) and represent the principal raw materials used for the production of the original vessels. The abundance of these minerals indicates that the raw materials were composed primarily of kaolinite and quartz, and that the firing temperatures did not exceed 600 °C, given that the presence of metakaolinite ($Al_2Si_2O_7$) indicates that the kaolinite in the raw material was converted into an amorphous phase. The structure of the kaolinite is ruptured during firing at 550 °C, but would have been transformed into mullite at a firing temperature of 950 °C (Evans and White, 1958) as noted in the TG/DTA curves (Fig. 3) which corroborates with the primary use of clays rich in kaolinite.

Kaolinite is the best suited mineral clay for the production of red ceramic, whether archeological or current production, both vessels manufactured as structural material (bricks and tiles) (Kukolev et al., 1972). Clays rich in kaolinite – sedimentary or weathered – are abundant throughout the Amazon region. The quartz associated with this mineral is also abundant, found in fine grains, but does not suffer alterations at the firing temperatures inferred for the samples analyzed in the present study.

The total chemical composition and spot measurements confirm that the basic raw material used for the production of the ceramics

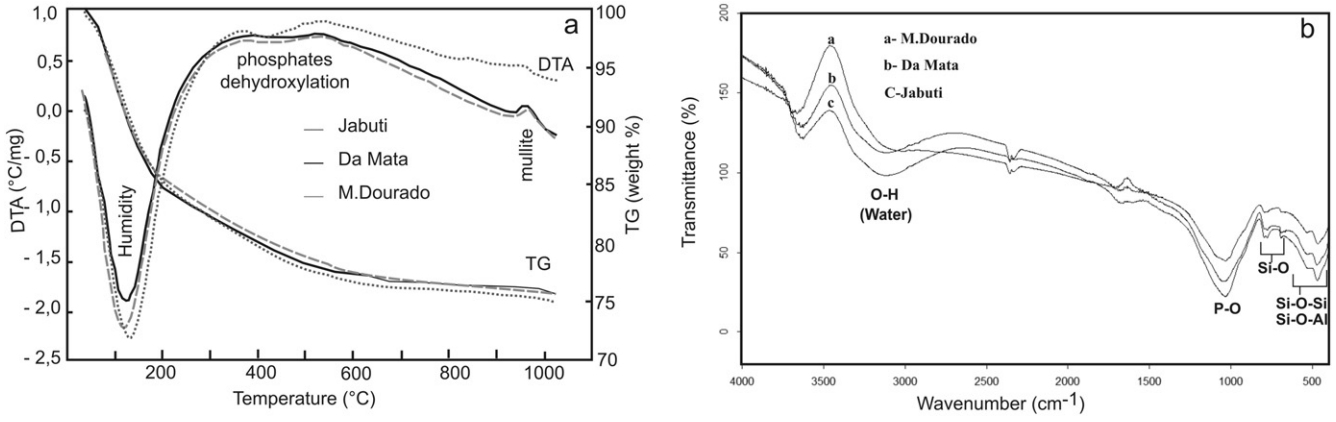

Fig. 4. a) Representative thermal analysis curves (TGA/DTG) of the sherds from Monte Dourado 1, Da Mata and Jabuti archeological sites. b) FT-IR of the sherds from Monte Dourado 1, Da Mata and Jabuti archeological sites showing the P–O bands.

Table 2
Chemical composition (major, minor elements and Loss on Ignition — LOI) of the sherds from Monte Dourado 1, Da Mata and Jabuti archeological sites.

Samples	SiO_2	Al_2O_3	Fe_2O_3	MgO	CaO	SrO	Na_2O	K_2O	TiO_2	P_2O_5	MnO	LOI	Total	n
	wt%													
	Monte Dourado 1													
CF-MD1 9 a	49.32	17.08	11.87	1.35	2.75	0.02	0.91	0.36	5.40	2.44	0.13	8.10	99.71	22
CF-MD1 12 b	44.37	16.60	19.09	2.12	3.14	0.02	0.83	0.25	7.32	1.40	0.25	4.20	99.57	3
CF-MD1 9 b	47.86	15.95	13.49	2.02	3.46	0.02	1.10	0.35	5.68	2.04	0.16	7.60	99.71	19
CF-MD1 12 b	46.83	16.29	15.07	2.20	3.69	0.02	1.08	0.52	4.68	1.49	0.17	7.70	99.72	3
CF-MD1 9 c	48.75	17.32	10.02	1.69	2.96	0.02	0.74	0.33	4.90	2.56	0.12	10.30	99.69	13
CF-MD1 12 c	51.29	13.96	13.66	2.31	3.73	0.02	1.13	0.32	4.09	1.17	0.15	7.90	99.71	3
CF-MD1 9 d	47.74	15.73	13.19	1.96	3.24	0.02	0.78	0.24	5.16	1.94	0.15	9.60	99.73	13
CF-MD1 12 d	42.20	15.26	15.76	1.64	2.83	0.01	0.61	0.08	6.03	2.17	0.16	12.90	99.64	4
CF-MD1 9 e	47.56	15.68	12.44	1.73	3.18	0.02	0.89	0.27	5.61	2.44	0.14	9.70	99.64	16
CF-MD1 12 e	40.39	18.69	14.45	2.90	4.49	0.02	1.15	0.24	4.90	2.86	0.16	9.40	99.63	4
CF-MD1 9 f	45.64	15.43	12.69	2.21	3.93	0.02	0.93	0.27	5.87	2.50	0.15	10.0	99.62	14
CF-MD1 12 f	49.31	16.14	11.17	1.94	3.80	0.02	1.09	0.29	4.57	2.55	0.13	8.70	99.69	4
CF-MD1 9 g	44.78	17.03	11.81	1.43	2.97	0.02	0.76	0.29	4.46	3.69	0.12	12.40	99.74	13
CF-MD1 12 g	47.52	17.49	11.58	2.25	4.43	0.02	1.28	0.29	2.90	1.93	0.14	9.90	99.71	5
CF-MD1 ≤ 9 mm[a]	**47.38**	**16.32**	**12.22**	**1.77**	**3.21**	**0.02**	**0.87**	**0.30**	**5.30**	**2.52**	**0.14**	**9.67**	**99.69**	**110**
CF-MD1 ≥ 12 mm[b]	**45.99**	**16.35**	**14.40**	**2.19**	**3.73**	**0.02**	**1.02**	**0.28**	**4.93**	**1.94**	**0.17**	**8.67**	**99.67**	**26**
Da Mata														
CF-DM 9 a	55.48	18.67	3.39	0.41	0.22	0.01	0.11	0.62	1.22	1.19	0.02	18.50	99.83	14
CF-DM 12 a	58.29	19.33	2.78	0.39	0.25	0.01	0.12	0.63	1.43	1.00	0.02	15.60	99.84	8
CF-DM 9 b	56.43	17.88	3.43	0.38	0.27	0.01	0.12	0.53	1.19	1.06	0.02	18.60	99.91	28
CF-DM 12 b	53.20	19.49	3.61	0.38	0.26	0.01	0.16	0.81	1.32	0.92	0.03	19.60	99.78	10
CF-DM 9 c	52.92	20.26	3.14	0.63	0.25	0.01	0.10	0.93	1.23	0.90	0.03	19.50	99.89	18
CF-DM 12 c	51.92	21.19	2.41	0.39	0.28	0.01	0.17	0.56	1.44	1.20	0.06	20.20	99.82	8
CF-DM 9 d	54.76	19.11	4.23	0.51	0.25	0.01	0.12	0.68	1.22	0.98	0.03	18.00	99.89	14
CF-DM 12 d	49.23	2244	2.52	0.35	0.24	0.01	0.09	0.43	1.45	1.31	0.02	21.80	99.88	12
CF-DM 9 e	60.16	15.81	4.86	0.65	0.34	0.01	0.15	0.80	0.95	0.78	0.08	15.30	99.88	16
CF-DM 12 e	53.69	20.13	2.79	0.35	0.21	0.01	0.12	0.66	1.41	1.09	0.01	19.40	99.86	9
CF-DM ≤9 mm[a]	**55.95**	**18.35**	**3.81**	**0.52**	**0.27**	**0.01**	**0.12**	**0.71**	**1.16**	**0.98**	**0.04**	**17.98**	**99.88**	**90**
CF-DM ≥ 12 mm[b]	**53.27**	**20.52**	**2.82**	**0.37**	**0.25**	**0.01**	**0.13**	**0.62**	**1.41**	**1.10**	**0.03**	**19.32**	**99.84**	**47**
Jabuti														
CF-JAB a	51.41	17.21	5.58	0.81	0.45	0.01	0.18	0.74	1.08	4.38	0.01	17.90	99.75	5
CF-JAB bc	54.31	17.13	5.91	0.53	0.62	0.02	0.19	0.90	1.08	6.40	0.01	12.70	99.78	4
CF-JAB de	39.62	20.11	4.59	0.37	0.97	0.04	0.10	0.52	1.10	7.64	0.03	24.70	99.75	4
CF-JAB fg	45.85	17.81	4.73	0.65	1.37	0.16	0.16	0.80	1.17	6.53	0.03	20.50	99.60	11
CF-JAB h	35.65	21.11	4.52	0.59	1.49	0.16	0.16	0.75	1.19	9.26	0.03	24.90	99.65	4
CF-JAB i	31.09	22.07	5.09	0.33	1.80	0.20	0.14	0.59	1.11	11.16	0.03	26.20	99.61	5
CF-JAB j	37.34	21.19	4.70	0.62	1.44	0.19	0.18	0.72	1.13	7.86	0.03	24.40	99.61	5
CF-JAB l	39.12	18.97	5.88	0.79	2.12	0.41	0.15	0.79	1.09	8.82	0.02	21.60	99.35	7
CF-JAB m	39.93	19.76	6.30	0.57	1.28	0.14	0.18	0.82	1.25	7.73	0.02	21.80	99.64	7
CF Jabuti[c]	**41.59**	**19.48**	**5.26**	**0.58**	**1.28**	**0.15**	**0.16**	**0.74**	**1.13**	**7.75**	**0.02**	**21.63**	**99.75**	**52**
CF Da Mata[c]	**54.61**	**19.43**	**3.32**	**0.44**	**0.26**	**0.01**	**0.13**	**0.67**	**1.29**	**1.04**	**0.03**	**18.65**	**99.86**	**137**
CF M. Dourado[c]	**46.68**	**16.33**	**13.31**	**1.98**	**3.47**	**0.02**	**0.95**	**0.29**	**5.11**	**2.23**	**0.15**	**9.17**	**99.68**	**136**
C. Porteira[d]	65.55	16.37	5.79	0.63	0.43	n.d.	0.69	0.9	0.86	2.37	0.01	n.d.	–	–
Manduquinha[e]	71.35	8.60	4.54	0.26	0.19	n.d.	0.98	0.59	0.4	1.31	0.01	11.63	99.86	–
Q Tacana[f]	56.53	17.36	3.43	0.42	0.04	n.d.	0.06	1.27	1.01	1.34	0.01	18.40	99.87	–
CCR[g]	64.90	14.60	4.40	4.12	2.24	374.6	3.46	3.45	0.52	0.15	0.07	n.d.	–	–
PAAS[h]	62.80	18.90	6.50	1.30	2.20	237.1	1.20	3.70	1.00	0.16	0.11	n.d.	–	–

n.d.: not determined; n: number of CF.
[a] Average of CF with thickness less than 9 mm.
[b] Average of CF thickness greater than 12 mm.
[c] Averege.
[d] Average of CF from Cachoeira-Porteira (Costa et al., 2004a).
[e] Average of CF from Manduquinha (Coelho et al., 1996).
[f] Average of CF from Quebrada Tacana (Costa et al., 2011).
[g] Continental crustal rock (Wedepohl., 1995).
[h] Post Archean Australian shale (Taylor and McLennan., 1985).

was an aluminosilicate, while the minor concentrations of K_2O in the Monte Dourado 1 samples (<0.3 wt.%) reflect the discreet presence of muscovite. In the Da Mata and Jabuti samples, the slightly higher concentrations of K_2O (0.4–0.8%) indicate the presence of muscovite or potassium feldspars, which would have been added as temper.

The levels of CaO (2.69–4.49% by weight) associated with those of Na_2O (0.6–1.28%) observed in the Monte Dourado 1 samples confirm the presence of plagioclases (Fig. 5a) of the labradorite type (mean CaO/Na_2O ratio = 3.7), identified as temper, whereas in the Da Mata samples, CaO and Na_2O were found at extremely low levels (Na_2O: <0.18%; CaO: <0.34%), confirming the absence of plagioclase. Relatively high levels of MgO were recorded at Monte Dourado 1 and represent cordierite, the only Mg mineral identified by XRD. While the levels of MgO recorded at Jabuti were still substantial (1.28%, on average), they were incompatible with the minerals identified by XRD of the samples from this site.

Similarly, high levels of TiO_2 were only recorded at Monte Dourado 1, and reflect the accessory status of ilmenite in the samples, as identified by XRD. In this case, the ilmenite + labradorite + cordierite + quartz + (muscovite) may correspond to fragments of metamorphosed mafic rock which was crushed and added to the basic clay as a non-plastic material. This eliminates the possible use of saprolite (clay with rock

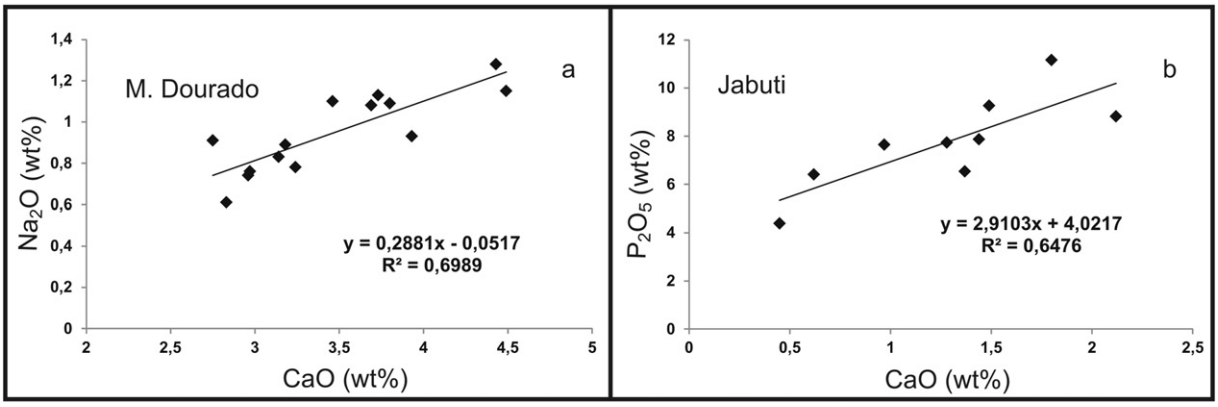

Fig. 5. a — Dispersion diagram showing the positive correlation between the CaO and Na_2O supporting the domain of the plagioclase labradorite in the samples from the Monte Dourado 1 site. b — Dispersion diagram showing a marked positive correlation between the CaO and P_2O_5 supporting the crandallite–goyazite domain in the Jabuti samples.

particles) derived from these rocks as a raw material, given that the plagioclases and cordierite are unable to resist typical tropical weathering.

4.2. Firing temperature

The firing temperature of the pots was estimated from the mineralogical transformations of the material. The amorphous metakaolinite domain shows that this temperature was higher than 550 °C, but did not reach 600 °C. This can be deduced from the presence of anatase, which would have been transformed into rutile at higher temperatures (Zhang et al., 2006). When calcined in the laboratory for 2 h at a temperature of 600 °C, the anatase is transformed into rutile.

The hematite may also be an important indicator of firing temperatures, although this mineral did not survive the long period of weathering in the ADE soils, and was reduced to iron hydroxides, which were probably amorphous, despite the high levels of Fe_2O_3 found in the analyses (Table 2). No crystalline phase of Fe was identified by XRD, except for ilmenite, which is resistant to weathering, and the rare mineral segelerite, found in the samples from Monte Dourado 1.

4.3. Neoformation after the manufacture of the vessels

The relatively high levels of CaO found in the Jabuti samples, independent of the Na_2O (<0.18%: Fig. 5b), and combined with the high values of SrO (≤0.16%), in addition to the high levels of P_2O_5, which respond to the presence of crandallite–goyazite, differentiate this site from the others. At Jabuti, this mineral substitutes pseudomorphically the shell fragments, which would normally be made up of calcite and/or aragonite, which indicates that the crandallite–goyazite was formed after the production of the ceramic pots, possibly during their daily use, and would thus not be a component of the ceramics.

Costa et al. (2006, 2011) related the phosphorus levels to the daily use of the pots for the preparation and storage of food, although Freestone et al. (1994) concluded that the concentrations in the ceramics were derived from the environment in which they were discarded, due to the micro-structure of the material, and were thus not an indicator of the use of the pots. The thinnest sherds (<9 mm) tended to have the highest concentrations of P_2O_5, however, which supports the conclusion that the enrichment of phosphorus was related primarily to the use of the post for cooking, as proposed by Costa et al. (2006, 2012). Schiffer et al. (1994), Rye (1981), and Braun (1983) all concluded that thin-walled pots were used for cooking food, given that they are better conductors of heat, and are more resistant to thermal shock.

The P_2O_5 content was no more than 11.16% (7.75%, on average) at Jabuti, much lower than the levels recorded at the other two sites. Even so, all the values are higher than those recorded in ceramic vessels retrieved from archeological sites in South Africa (0.007–1.18%) by Legodi and Waal (2007), and in Greece (0.08–0.21%) by Iordanidis et al. (2009) CCR and PAAS (Table 2; Fig. 6a). The lowest levels of P_2O_5 (1.04%, on average) were recorded in the sherds from Da Mata, although these values are similar to those recorded in studies of samples from other archeological sites in the Amazon region (Costa et al., 2009, 2011).

Like other hydroxylated or hydrated aluminum phosphates, crandallite–goyazite ($(Ca, Sr)Al_3(PO_4)_2(OH)_5$) is a mineral typical of hydrothermal environments (Schwab et al., 1990), equivalent to that found inside ceramic pots during the cooking of foods, as demonstrated by Costa et al. (2012). If this mineral was present in the raw material, it would not have resisted the inferred firing temperature, and if this temperature had been even higher, e.g., 900–1000 °C, the mineral would have been transformed into a crystalline phase, such as berlinite, and the metakaolinite, into mullite. These findings thus indicate that the aluminum phosphates were probably formed during the use of the pots to cook food, and would thus be important indicators of their use for the preparation of meals.

While the amorphous phosphates of aluminum or microcrystalline minerals such as crandallite–goyazite are derived from the use of the pots for cooking food, the segelerite identified in the sherds from Monte Dourado 1 (Fig. 2) indicates aerobic conditions, typical of flooded environments in which organic matter has accumulated. Under these conditions, the iron oxy-hydroxides in the sherds are partially dissolved by microbial activity, and the iron is reduced, as well as part of the amorphous aluminum phosphates, plagioclases, and the cordierite, which establishes ideal conditions for the precipitation of Ca–Mg–Fe phosphates, such as segelerite. The occurrence mode of the segelerite, partially replacing the aforementioned minerals, reinforces this conclusion.

The swampy conditions in the region of Monte Dourado 1 have persisted to the present day. Phosphates of Fe^{2+}, such as vivianite ($Fe_3(PO_4)_2 \cdot 8H_2O$) and mitridatite ($Ca_3Fe_4(PO_4)_4(OH)_6 \cdot 3H_2O$), have been identified in sherds (Maritan and Mazzoli, 2004), ferruginous lateritic crusts invaded by swamps (Costa and Lemos, 2000; Costa and Sa, 1980; Lemos et al., 2007) or even in swampy ground (Walpersdorf et al., 2013). Like the aluminum phosphates, these iron phosphates suffer thermal collapse (Fig. 4) at temperatures of over 400 °C (Hochleitner and Fehr, 2010). This means that these compounds could not have been part of the raw material, given the firing temperature of the ceramic vessels (550–600 °C).

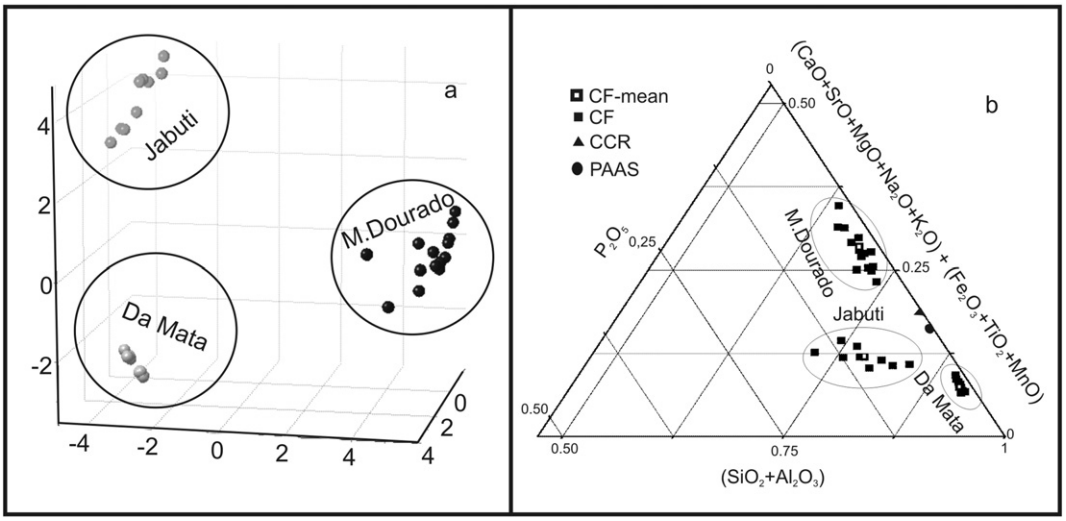

Fig. 6. a) XRD cluster analyses showing the clear distinction between the three sites; b) chemical diagrams discriminating the three sites based on the chemical composition of their sherds.

4.4. Provenience and discrimination of the sherds

The results of the chemical–mineralogical analyses of the sherds (Fig. 6a, b) emphasize the distinct characteristics of each group of samples, which probably reflects the different non-plastic materials (cariapé, shell, and crushed rock) used in the manufacturing process. Crushed metamorphic rocks in the Monte Dourado 1 sherds, and the large quantities of shell substituted by aluminum phosphates in the Jabuti sherds, contribute to the discrimination of the sherds from these sites.

Cariapé was the predominant temper at Da Mata, and the reduced levels of amorphous phosphates are clearly the component that distinguishes this site from the others. Overall, then, the chemical–mineralogical differences among the three sites reflect both the non-plastic materials used during the production process and the possible contamination by phosphates after the production of the pots.

The matrices of the Jabuti and Da Mata sherds were very similar in chemical terms (Table 1; Fig. 7 a, b), except of course in the levels of CaO, SrO, MgO, and P_2O_5, as well as their mineralogical composition, with the exception of the crandallite–goyazite found only at Jabuti. The higher values for SiO_2 recorded at Da Mata correspond to the abundance of cariapé, formed basically of SiO_2, both amorphous and in the form of tridymite–cristobalite. These similarities in the matrix used at the two sites are further reinforced by the distribution pattern of trace elements (Fig. 7a) and the rare earth elements normalized by the chondrites (Fig. 7b). The negative anomaly of Eu found in the present study is a characteristic of the material equivalent to granitoids and the products of weathering and the resulting aluminosilicate clays deposited in the lakes and alluvial plains found throughout the Amazon, which provided the raw materials for the manufacture of the pots.

The only divergent trace element was Sr, a potential component of shells and foods of marine origin. Calcium carbonates, such as aragonite, the principal component of recent shells, contain strontium (Findlater et al., 2014; Vonhof et al., 1998). The abundance of shell sherds and the coastal location of the Jabuti and Da Mata sites reinforce the relationship with this environment. The raw materials used at these sites were almost certainly derived from local geological deposits which, unlike those at Monte Dourado 1, are dominated by sedimentary rocks of the Barreiras Formation, primarily argillites made up of kaolinite, quartz, and illite/muscovite, as well as alluvial and lacustrine deposits of the coastal plains (Behling and Costa, 2004). On the other hand, the mineralogical assembly identified in the fragments from Monte Dourado 1 site can easily be associated with amphibolites that are part of the Ipitinga Group, the Paleo-Proterozoic geologic unit mapped near the study site (Vasquez et al., 2008).

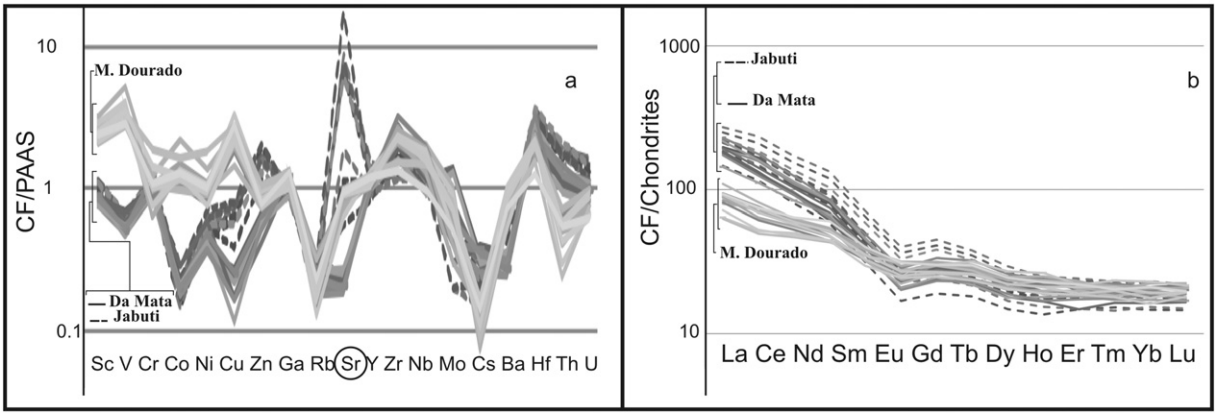

Fig. 7. a) Distribution of the contents of the trace elements found in the sherds, normalized by the PAAS; b) distribution of the REE in the sherds normalized by chondrites (Evensen et al., 1978).

5. Conclusions

The sherds analyzed from the three study sites presented distinct non-plastic material characteristics, which assign them to different groups. This discrimination was strongly supported by the presence and abundance of aluminum phosphates, in particular crandallite–goyazite, found primarily in the Jabuti and Da Mata samples. The Monte Dourado 1 site is distinguished from the others due to the use of metamorphosed mafic rocks mineralized into ilmenite, found in the area surrounding the study site. The presence of quartz may not necessarily be related to the use of non-plastic material, given that it is also a component of the clayey raw material.

Metakaolinite is the fundamental constituent of all the sherds, although the composition of the samples from Jabuti and Da Mata was the most similar. From a chemical viewpoint, the greatest differences were found in the levels of CaO, MgO, SrO, and P_2O_5, which reflect the neoformation of the phosphates and, in part, the shell temper. The levels of SiO_2, Al_2O_3, Fe_2O_3, and TiO_2 suggest the presence of argilites from the Barreiras Formation – the coastal region's dominant geological unit – as the raw material used for the ceramic matrix. The distribution of trace and rare earth elements reinforces these similarities. By contrast, it is possible that the raw materials for the ceramics produced at Monte Dourado 1 were clays derived from metamorphosed mafic rocks.

The firing temperature used in the production of the ceramic vessels was above 550 °C at all three sites, given the lack of kaolinite, although the presence of anatase in the Jabuti and Da Mata samples indicates that temperatures did not exceed 600 °C.

The aluminum phosphates found in the sherds indicate that the original pots were used to cook food, while the presence of segelerite in some samples suggests that the archeological site from which they were obtained was a hydromorphic (swampy) environment during some time in its history.

The chemical and mineralogical similarities and differences found among the sherds indicate the use of local raw materials, without the need for the exchange of raw materials among populations. The use of cariapé in most of the sherds reflects the widespread use of this resource, which may be an important indicator of prehistoric ceramic production in the Amazon region, despite the existence of a few exceptions.

Acknowledgements

We are grateful to the Brazilian National Research Council (CNPq), Brazilian Graduate Training Program (CAPES), Emilio Goeldi Paraense Museum (MPEG) and Scientia Scientific Consultants Ltd.

References

Alves, M.A., 1988. Análise cerâmica: estudo tecnotipológico. Ph.D. Thesis, Departamento de Antropologia da Faculdade de Filosofia, Letras e Ciências Humanas, Universidade de São Paulo (258 pp.).

Behling, H., Costa, M.L., 2004. Mineralogy, geochemistry, and palynology of modern and late tertiary mangrove deposits in the Barreiras Formation of Mosqueiro Island, northeastern Pará State, Eastern Amazonia. J. S. Am. Earth Sci. 17, 285–295.

Braun, D.P., 1983. Pots as tools. In: Moore, J.A., Keene, S.A. (Eds.), Archaeological Hammers and Theories. New York Academic Press, New York, pp. 107–134.

Breitinger, D.K., Brehm, G., Mohr, J., Colognesi, D., Parker, S.F., Stolle, A., Pimpl, Th.H., Schwab, R.G., 2006. Vibrational spectra of synthetic crandallite-type minerals — optical and inelastic neutron scattering spectra. J. Raman Spectrosc. 37, 208–216.

Coelho, S.R.C., Costa, M.L., Kern, D.C., 1996. Mineralogia e composição química dos fragmentos cerâmicos arqueológicos do sítio Manduquinha em Caxiuanã (Portel-Pa). SBG/NO, Simpósio de Geologia da Amazônia, Proceedings of the V Simpósio de Geologia da Amazonia, Belém, pp. 234–237.

Costa, M.L., Kern, D.C., 1999. Geochemical signatures of tropical soils with archaeological black earth in the Amazon, Brazil. J. Geochem. Explor. 66, 369–385.

Costa, M.L., Lemos, V.P., 2000. Siderita e vivianita em crostas lateríticas alteradas epigeneticamente (Padauari, Amazônia). Rev. Esc. Minas 2, 101–107.

Costa, M.L., Sa, J.H.S., 1980. Os fosfatos lateríticos da Amazônia Oriental: geologia, mineralogia, geoquímica e correlação com as bauxitas da Amazônia. Sociedade Brasileira de Geologia, Proceddings Congresso Brasileiro de Geologia. SBG, Camboriú, pp. 1459–1472.

Costa, M.L., Kern, D.C., Pinto, A.E., Souza, J.T., 2004a. The ceramic artifacts in Archaeological black earth (Terra Preta) from Lower Amazon Region, Brazil: chemistry and geochemical evolution. Acta Amazon. 34 (3), 375–386.

Costa, M.L., Kern, D.C., Pinto, A.H.E., Souza, J.R.T., 2004b. The ceramic artifacts in archaeological black earth (Terra Preta) from lower Amazon region, Brazil: mineralogy. Acta Amazon. 34 (2), 165–178.

Costa, M.L., Oliveira, E., Carmo, M.S., Kern, D.C., Göske, J., Raab, B., 2006. Origin of the phosphates in the ceramic artifacts from archaeological dark earth in the Lower Amazon Region. In: Rios, G.M., Camargo, S.M., Calvo, C.F. (Eds.), Pueblos y paisajes antiguos en la selva tropical. Universidad Instituto de Ciencias Naturales, Universidad Nacional de Colombia, Colombia, Bogota, pp. 311–323.

Costa, M.L., Carmo, M., Oliveira, H., Lima, H., Kern, D., Goeske, J., 2009. A Mineralogia e Composição Química de Fragmentos de Cerâmicas Arqueológicas em Sítios de Terra Preta de Índio. In: Teixeira, W.G., et al. (Eds.), As Terras Pretas de Índio da Amazônia: sua caracterização e uso deste conhecimento na criação de novas área. EMBRAPA Amazônia Ocidental, Manaus, pp. 225–241.

Costa, M.L., Rios, G.M., Silva, M.M.C., Silva, G.J., Valdes, U.M., 2011. Mineralogy and chemistry of archaeological ceramic fragments from archaeological dark earth site in Colombian Amazon. Rev. Esc. Minas 64 (1), 17–23.

Costa, M.L., Rodrigues, S.F.S., Silva, G.J., Pollmann, H., 2012. Crandallite formation in archaeological potteries found in the Amazonian dark earth soils. In: Broekmans, Maarten A.T.M. (Ed.), 1st ed. Proceedings of the 10th International Congress for Applied Mineralogy (ICAM) 1. Springer Verlag, Heidelberg (137-144 pp.).

Costa, J.A., Costa, M.L., Kern, D.C., 2013. Analysis of the spatial distribution of geochemical signatures for the identification of prehistoric settlement patterns in ADE and TMA sites in the lower Amazon Basin. J. Archaeol. Sci. 40, 2771–2782.

Dias, M.I., Prudêncio, M.I., Pinto De Matos, M.A., Luisa Rodrigues, A., 2013. Tracing the origin of blue and white Chinese Porcelain ordered for the Portuguese market during the Ming dynasty using INAA. J. Archaeol. Sci. 40, 3046–3057.

Evans, J.L., White, J., 1958. Further studies of the thermal decomposition (dehydroxilation) of clays. Br. Ceram. Trans. J. 57, 289–311.

Evensen, N.M., Hamilton, P.J., O'nions, R.K., 1978. Rare earth abundaces in chondritic meteorites. Geochim. Cosmochim. Acta 42, 1199–1212.

Fermo, P., Delnevo, E., Lasagni, M., Polla, S., Vos, M., 2008. Application of chemical and chemometric analytical techniques to the study of ancient ceramics from Dougga (Tunisia). Microchem. J. 88, 150–159.

Findlater, G., Shelton, A., Rolin, T., Andrews, J., 2014. Sodium and strontium in mollusc shells: preservation, palaeosalinity and palaeotemperature of the Middle Pleistocene of eastern England. Proceedings of the Geologists' Association 125, pp. 14–19.

Freestone, I., Middleton, A., Meeks, N., 1994. Significance of phosphate in ceramic bodies: discussion of paper by Bollong et al. J. Archaeol. Sci. 21, 425–426.

Gilkes, R.J., Palmer, B., 1983. Synthesis properties and dehidroxylation of members of the crandallite–goyazite series. Min. Mag. 47, 221–227.

Gimenez, R.G., Vigil De La Villa, R., Petit Domínguez, M.D., Rucandio, M.I., 2006. Application of chemical, physical and chemometric analytical techniques to the study of ancient ceramic oil lamp. Talanta 68, 1236–1246.

Glaser, B., Haumaier, L., Guggenberger, G., Zech, W., 2001. The Terra Preta phenomenon — a model for sustainable agriculture in the humid tropics. Naturwissenschaften 88, 37–41.

Hein, A., Day, M.P., Cau Ontiveros, M.A., Kilikoglou, V., 2004. Red clays from central and eastern Crete, geochemical and mineralogical properties in view of provenance studies on ancient ceramics. Appl. Clay Sci. 24, 245–255.

Hochleitner, R., Fehr, K.T., 2010. The keckite problem and its bearing on the crystal chemistry of the jahnsite group: mössbauer and electron-microprobe studies. Can. Mineral. 48, 1445–1453.

Iordanidis, A., Garcia-Guinea, J., 2011. A preliminary investigation of black, brown and red coloured potsherds from ancient upper Macedonia, northern Greece. MMA 11 (1), 85–97.

Iordanidis, A., Garcia-Guinea, J., Karamitrou-Mentessidi, G., 2009. Analytical study of ancient pottery from the archaeological site of Aiani, northern Greece. Mater. Charact. 60, 292–302.

Kern, D.C., Kämpf, N.O., 1989. Efeito de Antigos Assentamentos Indígenas na Formação de Solos com Terra Preta Arqueológica na Região de Oriximiná-Pa. Rev. Bras. Ciênc. Solo 13, 219–225.

Kramar, S., Lux, J., Mladenović, A., Pristacz, H., Mirtič, B., Sagadin, M., Rogan-Šmuc, M., 2012. Mineralogical and geochemical characteristics of Roman pottery from an archaeological site near Mošnje (Slovenia). Appl. Clay Sci. 57, 39–48.

Kukolev, G.G., Nemets, I.I., Semchenko, G.D., Belukha, G.D., Stanilov, B.E., Primachenko, V.V., 1972. Production dense ladle brick with a kaolin bond. Refractories 13, 216–218.

Legodi, M., Waal, D., 2007. Raman spectroscopic study of ancient South African domestic clay pottery. Spectrochim. Acta A 66, 135–142.

Lehmann, J., Kern, D.C., Glaser, B., Woods, W.I., 2003. Amazonian Dark Earths: Origin Properties Management. Springer (505 pp.).

Lemos, V.P., Costa, M.L., Lemos, R.L., De Faria, M.S., 2007. Vivianite and siderite in lateritic iron crust: an example of bioreduction. Quim. Nova 30, 36–40.

Lemos, V.P., Gurjão, R.S., Costa, M.L., 2011. Nutrients in Amazonian Black Earth from Caxiuanã region. J. Braz. Chem. Soc. 1, 1–5.

Lima, H.N., Schefer, C.E.R., Mello, J.W.V., Gilkes, R.J., Ker, J.C., 2002. Pedogenesis and pre-Colombian land use of "Terra Preta Anthrosols" (Indian Black Earth) of western Amazonia. Geoderma 110, 1–17.

Linné, S., 1925. The technique of South American ceramics. Göteborgs Kungl. Vetenskaps- och vitterhetssamhälles handlingar.

Madejová, J., Komadel, P., 2001. Baseline studies of the clay minerals society source clays: infrared methods. Clay Clay Miner. 49, 410–432.

Maritan, L., Mazzoli, Z., 2004. Phosphates in archaeological finds: implications for environmental conditions of burial. Archaeometry 46 (4), 673–683.

Maritan, L., Secco, M., Mazzoli, C., Mantovani, V., Bonetto, J., 2013. The decorated Padan terra sigillata from the site of Retratto, Adria (north-eastern Italy): provenance and production technology. Appl. Clay Sci. 82, 62–69.
Meggers, B., Evans, C., 1957. Archaeological investigations at the mouth of the Amazon. Bureau of American Ethnology, Washington (DC) (Bulletin 167).
Mescouto, C.S., Lemos, V.P., Dantas Filho, H.A., Costa, M.L., Kern, D.C., Fernandes, K.G., 2011. Distribution and availability of copper, iron, manganese and zinc in the archaeological black earth profile from the Amazon Region. J. Braz. Chem. Soc. 22, 1484–1492.
Mohamed, A., Janaki, K., Velraj, G., 2010. Microscopy, porosimetry and chemical analysis to estimate the firing temperature of some archaeological pottery shreds from India. Microchem. J. 95, 311–314.
Montana, G., Ontiveros, M.A.C., Polito, A.M., Azarro, E., 2011. Characterisation of clayey raw materials for ceramic manufacture in ancient Sicily. Appl. Clay Sci. 53, 476–488.
Moropoulou, A., Bakolas, A., Bisbikou, K., 1995. Thermal analysis as a method of characterizing ancient ceramic technologies. Thermochim. Acta 2570, 743–753.
Papadopoulou, D.N., Papadopoulou, D.N., Zachariadis, G.A., Tsirliganis, A.N., Anthemidis, N.C., Stratis, J.A., 2004. Comparison of a portable micro-X-ray fluorescence spectrometry with inductively coupled plasma atomic emission spectrometry for the ancient ceramics analysis. Spectrochim. Acta B 59, 1877–1884.
Prudêncio, M.I., Oliveira, F., Dias, M.I., Sequeira Braga, M.A., Delgado, M., Martins, M., 2006. Raw materials identification used for the manufacture of Roman "Bracarense" ceramics from NW Iberian Peninsula. Clay Clay Miner. 54 (5), 639–651.
Prudêncio, M.I., Dias, M.I., Gouveia, M.A., Marques, R., Franco, D., Trindade, M.J., 2009. Geochemical signatures of Roman amphorae produced in the Sado River estuary, Lusitania (Western Portugal). J. Archeol. Sci. 36, 873–883.
Rathossi, C., Pontikes, Y., 2010. Effect of firing temperature and atmosphere on ceramics made of NW Peloponnese clay sediments, part II. Chemistry of pyrometamorphic minerals and comparison with ancient ceramics. J. Eur. Ceram. Soc. 1853–1866.
Romani, A., Miliani, C., Morresi, A., Forini, N., Favaro, G., 2000. Surface morphology and composition of some "lustro" decorated fragments of ancient ceramics from Deruta Central Italy. Appl. Surf. Sci. 157, 112–122.
Rye, O.S., 1981. Pottery Technology: Principles and Reconstruction. Taraxacum. Manuals on archaeology, Washington, D.C.
Schiffer, M.B., Skibo, J.M., Belki, T.C., Neupert, M.A., Aronson, M., 1994. New perspectives on experimental archaeology: surface treatments and thermal response of the clay cooking pot. Am. Antiq. 59 (2), 197–217.
Schmidt, M.J., Py-Daniel, A.R., Moraes, C.P., Valle, R.B.M., Caromano, C.F., Teixeira, W.G., Barbosa, C.A., Fonseca, J.A., Magalhães, M.P., Santos, D.S.C., Silva, R.S., Guapindaia, V.L., Moraes, B., Lima, H.P., Neves, E.G., Heckenberger, M.J., 2014. Dark earths and the human built landscape in Amazonia: a widespread pattern of anthrosol formation. J. Archaeol. Sci. 42, 152–165.
Schwab, R.G., Herold, H., Götz, C., Oliveira, N.P., 1990. Compounds of the cradallite type: synthesis and properties of pure goyzite gorceixite and plumbogummite. Neues Jb. Mineral. Monat. H3, 113–126.
Scientia, 2009. Resgate dos sítios arqueológicos localizados na área da LT SL II – SL III. Relatório preliminar de Campo (15 pp.).
Scientia, 2011. Relatório parcial 3: Resgate de campo do sítio Monte Dourado 1. Projeto Arqueologia preventiva nas áreas de intervençãoda UHE Santo Antonio do Jari AP/PA (34 pp.).
Silveira, M.I., Oliveira, E.R., Kern, D.C., Costa, M.L., Rodrigues, S.F.S., 2011. O sítio Jabuti, em Bragança, Pará, no cenário arqueológico do litoral amazônico. Bol. Mus. Para. Emílio Goeldi. Cienc. Hum. 6, 335–346.
Simões, M.F., 1981. Coletores- pescadores ceramistas do litoral do Salgado. Bol. Mus. Para. Emílio Goeldi. 7, 1–33.
Smith, N.J.H., 1980. Anthrosols and human carrying capacity in Amazonia. Ann. Assoc. Am. Geogr. 70 (4), 553–566.
Taylor, R., McLennan, S.M., 1985. The Continental Crust: Its Composition and Evolution. Blackwell, Oxford (307 pp.).
Trindade, M.J., Dias, M.I., Coroado, J., Rocha, F., 2010. Firing tests on clay-rich raw materials from the Algarve Basin (South Portugal): study of the mineral transformations with temperature. Clay Clay Miner. 58, 188–204.
Trindade, M.J., Dias, M.I., Rocha, F., Prudêncio, M.I., Coroado, J., 2011. Bromine volatilization during firing of calcareous and non calcareous clays, archaeometric implications. Appl. Clay Sci. 53, 489–499.
Vasquez, M.L., Souza, C.S., Carvalho, J.M.A., 2008. Mapa geológico e de recursos minerais do estado do Pará, escala 1:1.000.000. In: Programa geologia do Brasil, integração, atualização e difusão de dados da geologia do Brasil, mapas geológicos estaduais. CPRM e Serviço geológico do Brasil, superintendência regional de Belém.
Vonhof, H.B., Wesselingh, Ł.F.P., Ganssena, G.M., 1998. Reconstruction of the Miocene western Amazonian aquatic system using molluscan isotopic signatures. Palaeogeogr. Palaeoclimatol. Palaeoecol. 141, 85–93.
Walpersdorf, E., Bender, K.C., Heiberg, L., O'Connell, D.W., Kjaergaard, C., Hansen, B.H.C., 2013. Does vivianite control phosphate solubility in anoxic meadow soils? Geoderma 193–194, 189–194.
Wedepohl, K.H., 1995. The composition of the continental crust. Geochim. Cosmochim. Acta 59, 1217–1232.
Woods, W.I., Teixeira, W.G., Lehmann, J., Steiner, C., WinklerPrins, A.M.G.A., Rebellato, L., 2009. Amazonian Dark Earths: Wim Sombroek's Vision. Springer.
Zhang, J., Li, M., Feng, Z., Chen, J., Li, C., 2006. UV Raman spectroscopic study on TiO_2. I. Phase transformation at the surface and in the bulk. J. Phys. Chem. B 110 (2), 927–935.